Journal of Applied Physics

RESEARCH ARTICLE | FEBRUARY 21 2024

Parallel pumping of magnons in inhomogeneous spin textures probed through NV spin relaxometry

J. Trimble ; B. Gould; F. J. Heremans ; S. S.-L. Zhang ; D. D. Awschalom ; J. Berezovsky

J. Appl. Phys. 135, 073904 (2024)
https://doi.org/10.1063/5.0192063

AIP Publishing

Journal of Applied Physics ARTICLE pubs.aip.org/aip/jap

Parallel pumping of magnons in inhomogeneous spin textures probed through NV spin relaxometry

Cite as: J. Appl. Phys. **135**, 073904 (2024); doi: 10.1063/5.0192063
Submitted: 18 December 2023 · Accepted: 29 January 2024 ·
Published Online: 21 February 2024

View Online Export Citation CrossMark

J. Trimble,[1] B. Gould,[1,2] F. J. Heremans,[3,4] S. S.-L. Zhang,[1] D. D. Awschalom,[3,4] and J. Berezovsky[1,a)]

AFFILIATIONS

[1]Department of Physics, Case Western Reserve University, Cleveland, Ohio 44106, USA
[2]Department of Physics, The Pennsylvania State University, University Park, Pennsylvania 16802, USA
[3]Pritzker School of Molecular Engineering, University of Chicago, Chicago, Illinois 60637, USA
[4]Center for Molecular Engineering and Materials Science Division, Argonne National Laboratory, Lemont, Illinois 60439, USA

[a)]**Author to whom correspondence should be addressed:** jab298@case.edu

ABSTRACT

We combine micromagnetic simulations and nitrogen-vacancy (NV) defect center spin relaxometry measurements to study magnon modes in inhomogeneous spin textures. A thin, micrometer-scale ferromagnetic disk is magnetized in a vortex state in which the magnetization curls around a central core. Micromagnetic simulations show that at zero applied field, the magnetization dynamics of the disk consist of a low frequency gyrotropic mode and higher frequency azimuthal magnon modes, all far detuned from the NV spin transition frequencies. An in-plane static magnetic field breaks the azimuthal symmetry of the vortex state, resulting in the magnon modes transforming in frequency and spatial profile as the field increases. Experimentally, we probe the dynamics of vortex magnetization as a function of applied in-plane static field and ac driving frequency by optically monitoring a nearby NV defect center spin. At certain values of the applied magnetic field, we observe enhanced spin relaxation when driving at twice the frequency of the NV ground state spin transition in optically detected magnetic resonance measurements. We attribute this effect to parallel pumping of a magnon mode in the disk producing magnons at half the excitation frequency. Micromagnetic simulations support this finding, showing spatial and spectral overlap of a confined magnon mode and an NV spin transition, with sufficient interaction strength to explain the observed signal.

I. INTRODUCTION

Single spin nitrogen-vacancy (NV) defect centers in diamond offer opportunities for high-sensitivity, nanoscale probing of magnons.[1–7] As an atomic-sized quantum sensor, NV centers allow for high spatial resolution measurements of magnon excitations confined in nanoscale dimensions within magnetic spin textures such as vortices, skyrmions, and magnetic domain wall structures. These spin textures are stable sources for short wavelength and nonlinear magnon generation which makes them attractive for applications in magnonic information processing and memory storage.[8–15]

In previous studies, NV defect center spins have been employed to study magnon phenomena in a range of magnetic thin films.[1–6] These experiments studied films with uniform magnetization and, with exception of Ref. 1, continuous magnon spectra. In magnetic films with continuous magnon spectra, through multi-magnon processes, excitation of magnon modes far detuned from the NV spin transitions results in spin relaxation. For example, driving the zero-wave-vector ferromagnetic (FM) resonance at frequencies below the NV spin transitions results in the excitation of a continuous band of magnon modes of higher wave-vector incoherent magnons, some of which are resonant with the NV spin transition frequencies. In the case of geometrically confined systems, the magnon mode spectrum becomes discrete, and NV spin relaxation is only observed when a magnon mode overlaps both in frequency with an NV spin transition and spatially with the NV defect.

In this experiment, we employ NV defect centers to study the discrete spectrum of magnon modes in a non-uniform magnetic

vortex. Thin, micrometer-scale FM disks with negligible anisotropy magnetize into a vortex ground state configuration. Figure 1(a) (inset) shows a simulation of the magnetization of a 2.1 μm diameter, 37 nm thick permalloy (Py) disk with no applied field. The magnetization curls around in the disk plane ($M_z = 0$), tangential to the disk boundary except in the center where the magnetization orients out-of-plane ($M_z \neq 0$). The central region with $M_z \neq 0$ is the vortex core with half width of $r_c = 10$ nm. As shown in Fig. 1(b) (inset), an external in-plane magnetic field $\vec{B} = (B_x, B_y)$ causes the disk magnetization to align with the field, shifting the vortex core perpendicularly with vortex core position $\vec{x} = (x, y) = c\chi_0(B_y, -B_x)$, where $c = \pm 1$ corresponds to vortex circulation clockwise or counterclockwise, and with $\chi_0 \approx 60$ nm/mT.[16] Here, $c = -1$ so that positive B_x yields displacement in positive y.

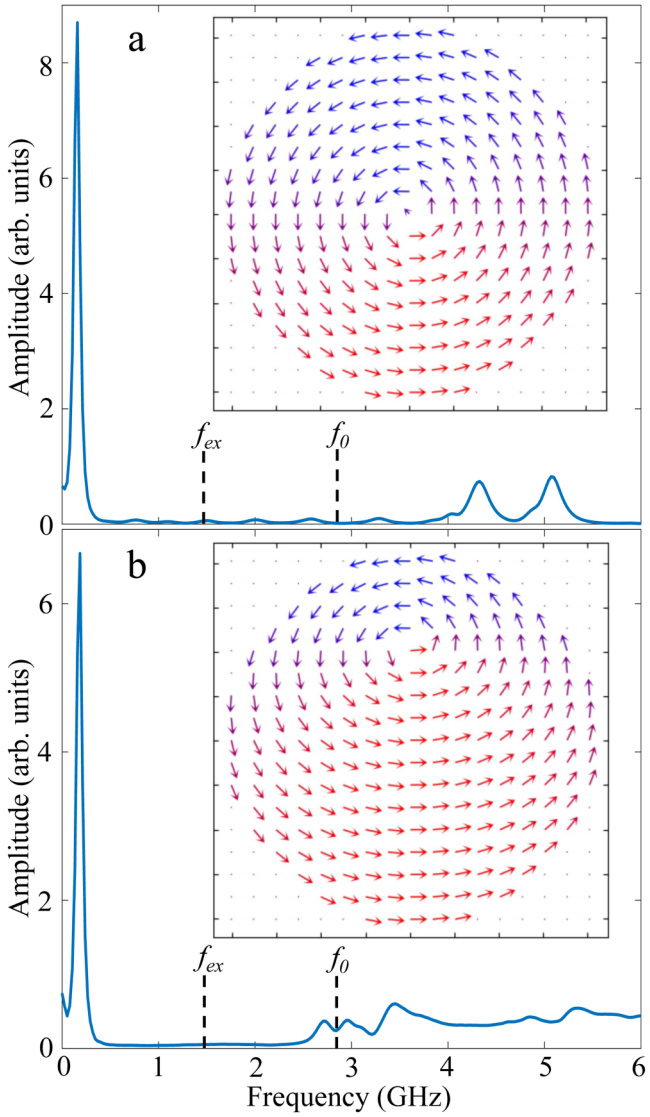

FIG. 1. (a) Simulated modes of a magnetic vortex Py disk at $\vec{B} = 0$ mT with simulated magnetization (inset). (b) Simulated modes of a magnetic vortex Py disk at $\vec{B} = (10, 0)$ mT with simulated magnetization (inset). The modes were excited through a broadband pulse.

These disks display a discrete spectrum of magnon modes with a frequency and spatial profile that depend on the magnetization state. For an unshifted vortex, the magnetization dynamics consist of confined azimuthal magnon modes which circulate around the entire disk at frequency $f_{az} = 4$–5 GHz, in addition to a low frequency soliton-like gyrotropic oscillation of the vortex core at $f_g = 0.16$ GHz. Figure 1(a) shows the frequency response of M_z averaged over the disk shown in the inset following a broadband pulse. We observe the gyrotropic mode at $f_g = 0.16$ GHz along with two azimuthal magnon modes at $f_{az} = 4.3$ and 5.1 GHz. These modes are well separated from the NV ground- and excited-state spin transition frequencies near f_0 and f_{ex}, respectively. As the vortex core shifts with an applied field $\vec{B}$, the azimuthal modes decrease in frequency and become confined in local regions of the disk.[17] Figure 1(b) shows the frequency response of M_z for the disk depicted in the inset. The azimuthal modes have shifted in frequency and now overlap the NV ground state spin transitions.

The evolution of these modes with field can be understood by looking at their spatial profile.[17] Figure 2 shows the response of $\vec{M}$ at a single frequency, as a function of position. The color intensity of the plot represents amplitude of magnetization response while the color represents the phase. With no field applied, the azimuthal modes at $f_{az} = 4.3$ and 5.1 GHz traverse the entire disk as shown in Figs. 2(a) and 2(b). These modes are counterpropagating and one revolution represents a phase increase of 2π. The azimuthal modes only survive in the low-field regime, however. As a static field $\vec{B}$ is applied, the magnon modes become localized in potential wells on either side of the vortex core due to build up of magnetic charges around the vortex core and disk edges.[15] Figure 2 shows the spatial profile of locally confined magnon modes at $\vec{B} = 10$ mT and frequency f of (c) 2.78 and (d) 2.97 GHz. These modes appear as standing waves confined locally in lobes on each side of the disk.[18]

II. MATERIALS AND METHODS

The next two paragraphs describe the experimental process used in this paper as reported previously.[7]

A layer of isotopically pure ^{12}C was grown on an electronic-grade single crystal diamond (Element Six) via plasma enhanced chemical vapor deposition. $^{15}N_2$ gas was introduced into the growth process at the appropriate time to achieve a 15 nm deep delta-doped layer of nitrogen. A subsequent electron irradiation (2 MeV, 1e14 dose) was used to create the vacancies followed by annealing of the sample at 850°C under forming gas (H_2/Ar) for 2 h to form the NV centers. A triacid ($HClO_4$:HNO_3:H_2SO_4) clean was then used to remove residual contaminants from the sample surface. Details about the processing and growth of the NV defect center-containing diamond film can be found in Refs. 19–21. An array of 2.1-μm diameter and 37-nm thick Py disks were then fabricated atop the NV center-containing diamond film by electron beam lithography, electron beam evaporation, and liftoff. This

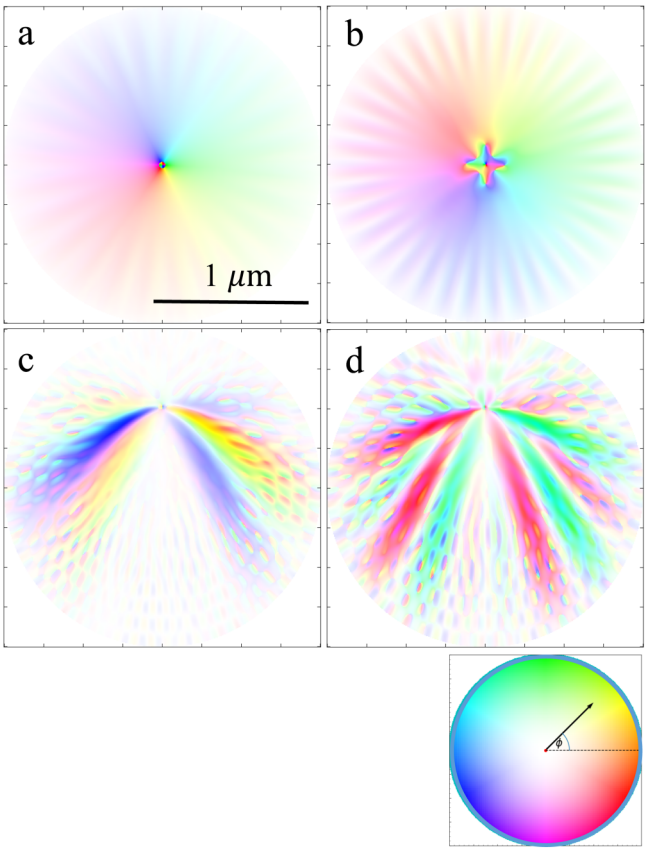

FIG. 2. Simulated spatial profile of azimuthal modes due to a broadband pulse in Py disk at $\vec{B} = 0$ mT and frequency f_{az} of (a) 4.3 and (b) 5.1 GHz. Simulated spatial profile of locally confined modes due to a broadband pulse in Py disk at $\vec{B} = 10$ mT and frequency f of (c) 2.78 and (d) 2.97 GHz. Bottom right shows the hue/saturation color scale used in other panels mapping the amplitude (saturation) of the Fourier components of $\vec{M}$ and phase angle (hue) of the Fourier component of M_z at the indicated frequencies. Scale bar is the same in all panels.

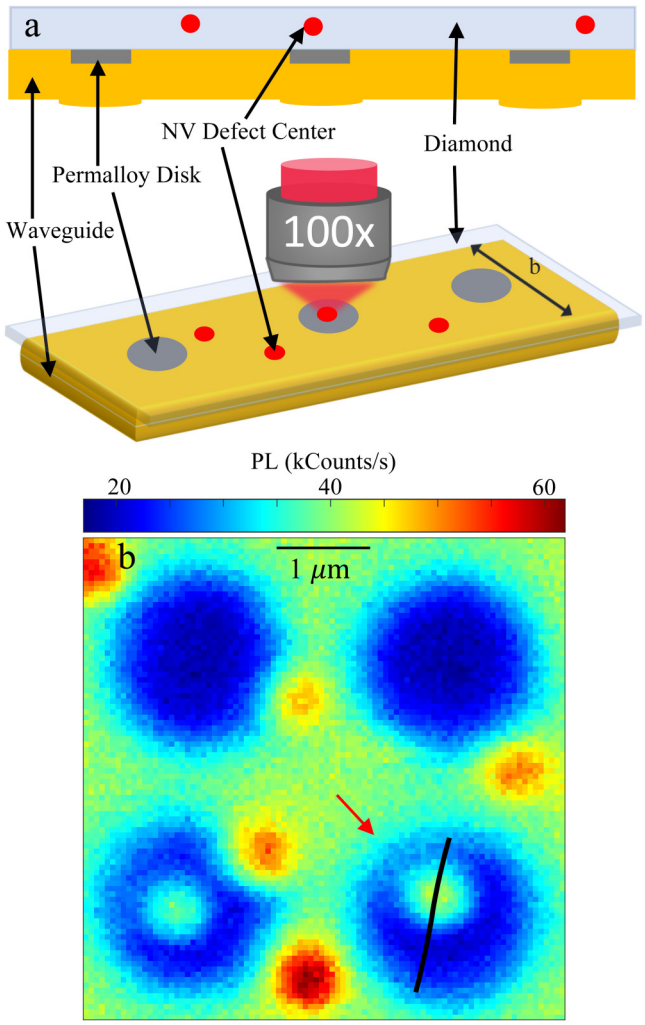

FIG. 3. (a) Sample schematic. (b) Scanning PL image of four disks (blue) with several nearby NV defects (bright spots). The disk/NV pair used here is indicated by the red arrow. The calculated path of the vortex core over the range of $B_0 = -12$ to 12 mT is shown by the black line. Scale bar = 1 μm.

results in a 15 nm vertical separation between the surface of the disks and the NV centers. A subsequent photo-lithography process was used to pattern a 125 nm thick gold co-planar waveguide (CPW) over the disk array. Figure 3(a) shows a schematic of the sample and setup. A 100× oil immersion microscope with 1.25 numerical aperture focuses 532-nm-wavelength excitation onto the sample from the back side of the diamond. Photoluminescence (PL) is collected back through the objective and detected by a single photon counting module. Figure 3(b) shows a scanning PL image of four Py disks (blue), with several NV centers (bright spots) in the diamond ≈ 15 nm above the disks. The NV/disk pair studied in this paper is indicated by the red arrow.

In the small magnetic fields $\vec{B}$ here, transitions from $m_s = 0$ to the $m_s = \pm 1$ sublevels occur at $f_\pm \approx f_{zfs} \pm (\gamma/2\pi)\vec{B} \cdot \hat{n}$, where $\hat{n}$ is the axis of the NV defect and $f_{zfs} = f_0$ or f_{ex} for the orbital ground and excited states, respectively. The gyromagnetic ratio $\gamma/2\pi = 28$ MHz/mT. To produce optically detected magnetic resonance (ODMR) spectra, a microwave magnetic field $b = 0.7$ mT is applied by driving the CPW at a frequency f_{ac} while the PL intensity is monitored. The value of b at the position of the NV and vortex is calculated from the measured current in the CPW and the CPW geometry. Via an arrangement of permanent magnets on motorized stages, an in-plane static magnetic field $\vec{B}$ both splits the spin transitions and also sets the position of the vortex core within the disk. We sweep the vortex core along the line shown in black in Fig. 3(b) by applying a field $\vec{B} = \vec{B}_{off} + B_0\hat{l}$, where $\vec{B}_{off} = -1.3$ mT is constant and B_0 is swept along an axis $\hat{l}$ oriented at approximately 45° with respect to the direction of b. We collect ODMR spectra at different B_0, mapping out NV spin polarization as a function of the interaction with the magnetization of the disk and

the applied field. In practice, we collect the data in two sweeps starting from $B_0 = 0$ in the negative and positive directions. In all cases, we do not ramp $|B_0| > 12$ mT to avoid annihilation and re-formation of the vortex state.

III. RESULTS

Figure 4 shows the ODMR spectrum f_{ac} vs B_0 of a single NV defect center over a magnetic vortex disk as shown in Fig. 3(b). The resonances centered around f_0 show the NV center ground state transitions under the influence of the applied magnetic field and the dipolar fringe field of the magnetic vortex.[22] In the region $B_0 \approx 0$ to 8 mT, the NV center ground state transitions centered at f_0 display strong and irregular splitting due to the proximity of the vortex core. Outside of this region ($B_0 < 0$ and $B_0 > 8$ mT), the transitions show nearly linear Zeeman splitting into two branches f_+ and f_-, with some asymmetry due to longer range fringe fields emanating from the magnetic texture of the vortex. The high frequency ODMR contrast labeled f_H and highlighted by red dashed boxes is the subject of this paper and discussed further below. Additionally, we observe intermittent ODMR contrast at $f_g = 0.15$ GHz due to the vortex core gyrotropic mode.[7] The cause of the broad features near f_0 and f_{ex} at $B_0 = 2$–7 mT is not identified.

Simulated magnon spectra f vs B_0 for a 2.1 μm diameter, 37 nm thick Py disk under static bias field $B_0 = -12$ to 12 mT are shown in Fig. 5. Simulations are carried out using the object-oriented micromagnetic framework (OOMMF[23]), with a $5.25 \times 5.25 \times 9.25\ \text{nm}^3$ cell size. Values $M_s = 8.1 \times 10^5$ A/m, $\alpha = 0.008$, and $A = 1.05 \times 10^{-11}$ J/m are used for the saturation magnetization, Gilbert damping coefficient, and exchange stiffness, respectively. Excitation is provided by a broadband magnetic field pulse $b_p = b_0 \text{sinc}(\pi \nu_p t)$, where $b_0 = 1$ mT and $\nu_p = 20$ GHz. The subsequent magnetization dynamics are recorded, with the frequency response extracted by performing FFTs of $\vec{M}$ vs time at each position. At $B_0 = 0$, we observe the gyrotropic mode $f_g = 0.16$ GHz and the azimuthal mode doublets 1 and 2 at $f_{az} = 5.1$ and 4.3 GHz. As the magnetic field B_0 is increased, we observe mode 2 shift to higher frequency while mode 1 remains constant before becoming suppressed at higher B_0. The gyrotropic mode $f_g = 0.16$ GHz remains constant over the entire field range. New magnon modes 3 and 4 emerge with increasing B_0 and shift to lower f. NV ground state resonances f_+ and f_- extracted from Fig. 4 are plotted over the simulated data as red and green circles to compare with the modes of the disk. Also plotted are the high

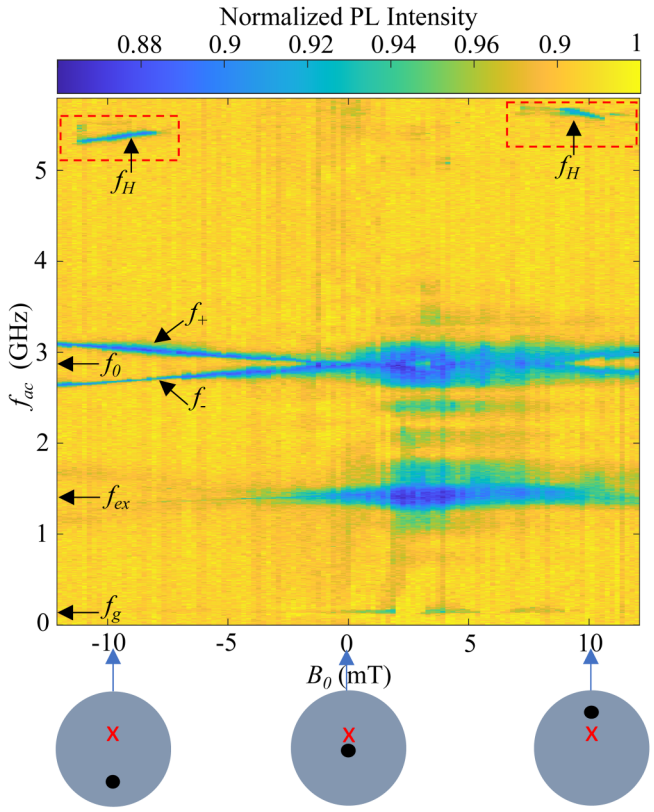

FIG. 4. ODMR spectra f_{ac} vs B_0 of the NV spin above a magnetic vortex. The features at f_H are highlighted by a red dashed box. Diagrams at the bottom illustrate the position of the vortex core (black dot) relative to the NV center (red ×) at three values of B_0.

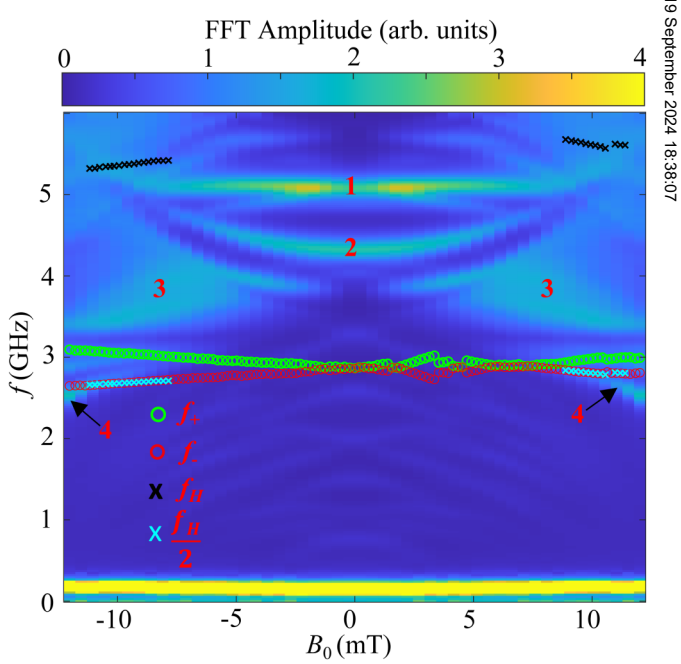

FIG. 5. Simulated modes f vs B_0 of a magnetic vortex with experimental ODMR resonances added. The yellow bands are simulated modes of the magnetic disk and the green and red circles are the NV ground state resonances f_+ and f_- from Fig. 4. The black x data points are the resonances at f_H in the ODMR data, also plotted at $\frac{f_H}{2}$ (blue) to compare with f_-.

frequency ODMR resonances f_H along with $\frac{f_H}{2}$ for comparison with f_-.

The high frequency ODMR features f_H observed in Fig. 4 are not expected in our spectrum. There are no NV spin resonances in this region and no known resonant modes of the magnetic vortex that would explain them. The off-resonant contrast f_H, however, appears at exactly twice the frequency f_- of an NV ground state spin transition. This suggests parallel pumping as a mechanism to explain the off-resonant ODMR contrast. In the phenomenon of parallel pumping, an AC driving field f_{ac}, applied parallel to the magnetization of a thin magnetic film, efficiently excites magnons at $\frac{f_{ac}}{2}$.[24] Given the inhomogeneous magnetization of the magnetic vortex, parallel pumping is likely to occur in general.

To support the hypothesis of parallel pumping, we compare the observed field range of the features at f_H to the magnon mode crossings of f_- in the simulated magnon spectra. Next, we show

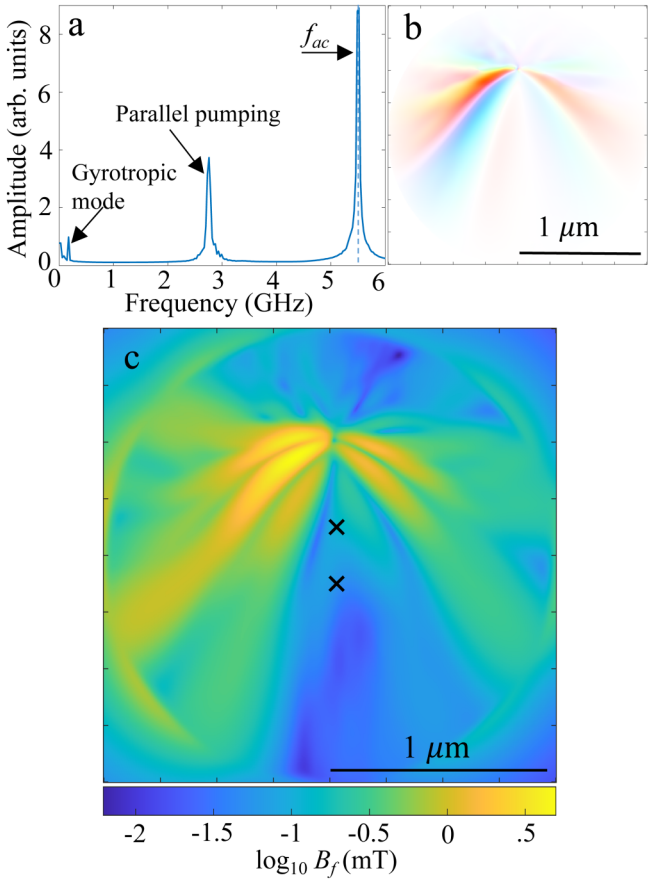

FIG. 6. (a) Simulated Fourier amplitudes of a magnetic vortex excited with a narrowband pulse of $f_{ac} = 5.5$ GHz with $B = 10$ mT. (b) Simulated spatial profile of parallel pumped mode at $\frac{f_{ac}}{2} = 2.75$ GHz in (a). (c) Simulated demagnetization field 30 nm above the disk in (b). The black "×" marks in (c) show the location of the NV center from our experiment with the lower "×" representing the location of the NV center at $B = -10$ mT. Scale bar = 1 μm.

through further time-domain simulations that driving at f_H results in parallel pumping of the mode at f_-. Last, we will show the magnetic fringe field produced by this mode overlaps spatially with the NV center with magnitude sufficient to create ODMR contrast.

The key element of our results showing off-resonant NV spin relaxation due to overlap of a confined magnon mode with a spin resonance is shown in Fig. 5. Magnon mode 4 crosses the NV ground state transition f_- over the same magnetic field ranges B_0 where we observe the ODMR features f_H (indicated by black "×" symbols). As noted above, $\frac{f_H}{2}$ (indicated by blue "×" symbols) falls exactly along the curve f_- as shown in Fig. 5, even tracking a small jump in f_- at $B_0 = 10.7$ mT, which is caused by vortex pinning.[22] This is the hallmark of parallel pumping where driving at frequency f produces magnons at $\frac{f}{2}$, for example, as observed in Ref. 25 in continuous YIG magnetic insulator films. This result is in contrast to three-magnon scattering in a magnetic vortex where excitation of radial modes decay into two azimuthal modes at $\frac{f}{2} \pm \Delta f$.[13,26]

We confirm that a parallel pumping process occurs in our magnetic disk by performing additional micromagnetic simulations at $B_0 = 10$ mT with continuous single-frequency excitation at $f_{ac} = 5.5$ GHz and the same amplitude used in the experiment. The frequency response of the simulation is shown in Fig. 6(a) as the average of the Fourier amplitude of M_z. The peak appearing at $f_{ac} = 5.5$ GHz is resonant with the driving field. A second peak appears at $\frac{f_{ac}}{2} = 2.75$ GHz, which is the expected parallel pumping effect. The spatial profile of the response at $\frac{f_{ac}}{2} = 2.75$ GHz is plotted in Fig. 6(b) and closely resembles the profile of magnon mode 4, as shown in Fig. 2(c). The small feature $f_g = 0.17$ in Fig. 5 (a) corresponds to the vortex core gyrotropic mode which is being weakly excited off resonance either by coupling to the parallel pumped mode at $\frac{f_{ac}}{2} = 2.75$ GHz, by the driving field $f_{ac} = 5.5$ GHz, or by both.

We further verify that the magnetic fringe field produced by parallel pumping of mode 4 is sufficient to explain the off-resonant ODMR contrast f_H observed in Fig. 4. The amplitude of the simulated demagnetization field above the disk created by the parallel pumped magnon mode $\frac{f_{ac}}{2}$ is shown in Fig. 6(c). The upper black "×" marks the location of the NV center in our experiment with the lower "×" equivalent to a simulation at $B_0 = -10$ mT but with the disk rotated 180°. We observe spatial overlap between the magnetic field and NV center in both configurations with amplitude $B_f \approx 0.1$ mT which is the same order of magnitude as the experiment where $b = 0.7$ mT and sufficient to explain the off-resonant ODMR contrast.

IV. DISCUSSION

Though one would also expect resonant pumping of magnon mode 4, we cannot conclusively identify resulting features in the ODMR data. From our simulation results, we estimate that the parallel pumping efficiency is ~ 50% of the resonant pumping efficiency of mode 4. The linewidth and amplitude of the f_+ and f_- resonances in Fig. 4 vary with B_0 due to the combination of the driving field b and the response of the vortex to that driving field. Due to the chirality of the vortex state, the response of the vortex may couple differently to f_+ and f_- and may add constructively or destructively to driving field itself.[27] Given the complexity of the

spatial profile of the fringe field, it is difficult to ascribe particular features to interactions with particular modes.

We have demonstrated coupling of a confined magnon mode in a shifted magnetic vortex to an NV defect spin through a parallel pumping process. Despite driving the ac field at frequencies far detuned from an NV spin transition, we observe enhanced spin relaxation when an in-plane magnetic bias field is applied to an FM disk. The off-resonant spin relaxation results from parallel pumping of a magnon mode at half the frequency of excitation. Unlike three-magnon scattering in radially excited vortices, parallel pumping creates pairs of phase connected magnons at exactly half the frequency of excitation. Nonlinear magnon processes in vortices such as those observed here have potential for applications in neuromorphic[12,13] and reservoir[14,15] computing. NV defect centers open a path for probing of highly localized magnon excitations confined in nanoscale regions of non-uniform magnetization. The technique could be extended for detailed mapping of complex spin textures such as skyrmions, vortices, and magnetic domain walls, with additional spatial information potentially obtained through a scanning NV approach.

ACKNOWLEDGMENTS

We acknowledge support from the National Science Foundation (NSF) (Award No. 2326528). Work supported in part (D.D.A. and F.J.H.) by Q-NEXT, a U.S. Department of Energy Office of Science National Quantum Information Science Research Center. Work by S.S.-L. Zhang was also partly supported by the College of Arts and Sciences, Case Western Reserve University. Simulations were performed on the Pennsylvania State University's Institute for Computational and Data Sciences' Roar supercomputer with the code developed and tested by using the High Performance Computing Resource in the Core Facility for Advanced Research Computing at Case Western Reserve University.

AUTHOR DECLARATIONS

Conflict of Interest

The authors have no conflicts to disclose.

Author Contributions

J. Trimble: Investigation (lead); Writing – original draft (lead). **B. Gould:** Investigation (supporting); Software (lead); Visualization (lead); Writing – review & editing (supporting). **F. J. Heremans:** Investigation (supporting). **S. S.-L. Zhang:** Formal analysis (lead); Supervision (equal); Writing – review & editing (supporting). **D. D. Awschalom:** Funding acquisition (equal); Supervision (equal). **J. Berezovsky:** Conceptualization (lead); Funding acquisition (equal); Supervision (equal); Writing – review & editing (lead).

DATA AVAILABILITY

The data that support the findings of this study are available from the corresponding author upon reasonable request.

REFERENCES

[1]T. Van Der Sar, F. Casola, R. Walsworth, and A. Yacoby, "Nanometre-scale probing of spin waves using single-electron spins," Nat. Commun. **6**, 7886 (2015).
[2]M. R. Page, B. A. McCullian, C. M. Purser, J. G. Schulze, T. M. Nakatani, C. S. Wolfe, J. R. Childress, M. E. McConney, B. M. Howe, P. C. Hammel, and V. P. Bhallamudi, "Optically detected ferromagnetic resonance in diverse ferromagnets via nitrogen vacancy centers in diamond," J. Appl. Phys. **126**, 124902 (2019).
[3]B. A. McCullian, M. Chilcote, V. P. Bhallamudi, C. M. Purser, E. Johnston-Halperin, and P. C. Hammel, "Broadband optical detection of ferromagnetic resonance from the organic-based ferrimagnet V[TCNE]$_x$ using N-V centers in diamond," Phys. Rev. Appl. **14**, 024033 (2020).
[4]B. A. McCullian, A. M. Thabt, B. A. Gray, A. L. Melendez, M. S. Wolf, V. L. Safonov, D. V. Pelekhov, V. P. Bhallamudi, M. R. Page, and P. C. Hammel, "Broadband multi-magnon relaxometry using a quantum spin sensor for high frequency ferromagnetic dynamics sensing," Nat. Commun. **11**, 5229 (2020).
[5]E. Lee-Wong, R. Xue, F. Ye, A. Kreisel, T. van der Sar, A. Yacoby, and C. R. Du, "Nanoscale detection of magnon excitations with variable wavevectors through a quantum spin sensor," Nano Lett. **20**, 3284–3290 (2020).
[6]P. Andrich, C. F. de las Casas, X. Liu, H. L. Bretscher, J. R. Berman, F. J. Heremans, P. F. Nealey, and D. D. Awschalom, "Long-range spin wave mediated control of defect qubits in nanodiamonds," npj Quantum Inf. **3**, 28 (2017).
[7]J. Trimble, B. Gould, F. J. Heremans, S. S.-L. Zhang, D. D. Awschalom, and J. Berezovsky, "Relaxation of a single defect spin by the low-frequency gyrotropic mode of a magnetic vortex," J. Appl. Phys. **130**, 083903 (2021).
[8]A. Barman, G. Gubbiotti, S. Ladak, A. O. Adeyeye, M. Krawczyk, J. Gräfe, C. Adelmann, S. Cotofana, A. Naeemi, V. I. Vasyuchka, B. Hillebrands, S. A. Nikitov, H. Yu, D. Grundler, A. V. Sadovnikov, A. A. Grachev, S. E. Sheshukova, J.-Y. Duquesne, M. Marangolo, G. Csaba, W. Porod, V. E. Demidov, S. Urazhdin, S. O. Demokritov, E. Albisetti, D. Petti, R. Bertacco, H. Schultheiss, V. V. Kruglyak, V. D. Poimanov, S. Sahoo, J. Sinha, H. Yang, M. Münzenberg, T. Moriyama, S. Mizukami, P. Landeros, R. A. Gallardo, G. Carlotti, J.-V. Kim, R. L. Stamps, R. E. Camley, B. Rana, Y. Otani, W. Yu, T. Yu, G. E. W. Bauer, C. Back, G. S. Uhrig, O. V. Dobrovolskiy, B. Budinska, H. Qin, S. van Dijken, A. V. Chumak, A. Khitun, D. E. Nikonov, I. A. Young, B. W. Zingsem, and M. Winklhofer, "The 2021 magnonics roadmap," J. Phys.: Condens. Matter **33**, 413001 (2021).
[9]V. S. Pribiag, I. N. Krivorotov, G. D. Fuchs, P. M. Braganca, O. Ozatay, J. C. Sankey, D. C. Ralph, and R. A. Buhrman, "Magnetic vortex oscillator driven by d.c. spin-polarized current," Nat. Phys. **3**, 498 (2007).
[10]X. Zhang, M. Ezawa, and Y. Zhou, "Magnetic skyrmion logic gates: Conversion, duplication and merging of skyrmions," Sci. Rep. **5**, 9400 (2015).
[11]S. Parkin and S.-H. Yang, "Memory on the racetrack," Nat. Nanotechnol. **10**, 195–198 (2015).
[12]L. Körber, K. Schultheiss, T. Hula, R. Verba, J. Fassbender, A. Kákay, and H. Schultheiss, "Nonlocal stimulation of three-magnon splitting in a magnetic vortex," Phys. Rev. Lett. **125**, 207203 (2020).
[13]L. Körber, C. Heins, I. Soldatov, R. Schäfer, A. Kákay, H. Schultheiss, and K. Schultheiss, "Modification of three-magnon splitting in a flexed magnetic vortex," Appl. Phys. Lett. **122**, 92401 (2023).
[14]D. Pinna, G. Bourianoff, and K. Everschor-Sitte, "Reservoir computing with random skyrmion textures," Phys. Rev. Appl. **14**, 054020 (2020).
[15]L. Körber, C. Heins, T. Hula, J.-V. Kim, S. Thlang, H. Schultheiss, J. Fassbender, and K. Schultheiss, "Pattern recognition in reciprocal space with a magnon-scattering reservoir," Nat. Commun. **14**, 3954 (2023).
[16]J. Trimble and J. Berezovsky, "Barkhausen imaging: A magneto-optical approach to mapping the pinning landscape in soft ferromagnetic films," J. Magn. Magn. Mater. **523**, 167585 (2021).
[17]F. G. Aliev, J. F. Sierra, A. A. Awad, G. N. Kakazei, D.-S. Han, S.-K. Kim, V. Metlushko, B. Ilic, and K. Y. Guslienko, "Spin waves in circular soft magnetic dots at the crossover between vortex and single domain state," Phys. Rev. B **79**, 174433 (2009).

[18]A. S. Jenkins, L. S. E. Alvarez, S. Memshawy, P. Bortolotti, V. Cros, P. P. Freitas, and R. Ferreira, "Electrical characterisation of higher order spin wave modes in vortex-based magnetic tunnel junctions," Commun. Phys. **4**, 107 (2021).
[19]K. Ohno, F. J. Heremans, L. C. Bassett, B. A. Myers, D. M. Toyli, A. C. B. Jayich, C. J. Palmstrøm, and D. D. Awschalom, "Engineering shallow spins in diamond with nitrogen delta-doping," Appl. Phys. Lett. **101**, 082413 (2012).
[20]K. Ohno, F. J. Heremans, C. F. de las Casas, B. A. Myers, B. J. Alemán, A. C. B. Jayich, and D. D. Awschalom, "Three-dimensional localization of spins in diamond using ^{12}C implantation," Appl. Phys. Lett. **105**, 052406 (2014).
[21]H. J. Mamin, M. H. Sherwood, M. Kim, C. T. Rettner, K. Ohno, D. D. Awschalom, and D. Rugar, "Multipulse double-quantum magnetometry with near-surface nitrogen-vacancy centers," Phys. Rev. Lett. **113**, 030803 (2014).
[22]M. S. Wolf, R. Badea, and J. Berezovsky, "Fast nanoscale addressability of nitrogen-vacancy spins via coupling to a dynamic ferromagnetic vortex," Nat. Commun. **7**, 11584 (2016).
[23]The code is available at http://math.nist.gov/oommf.
[24]T. Brächer, P. Pirro, and B. Hillebrands, "Parallel pumping for magnon spintronics: Amplification and manipulation of magnon spin currents on the micron-scale," Phys. Rep. **699**, 1–34 (2017).
[25]E. Lee-Wong, R. Xue, F. Ye, A. Kreisel, T. Van Der Sar, A. Yacoby, and C. R. Du, "Nanoscale detection of magnon excitations with variable wavevectors through a quantum spin sensor," Nano Lett. **20**, 3284 (2020).
[26]K. Schultheiss, R. Verba, F. Wehrmann, K. Wagner, L. Körber, T. Hula, T. Hache, A. Kákay, A. A. Awad, V. Tiberkevich, A. N. Slavin, J. Fassbender, and H. Schultheiss, "Excitation of whispering gallery magnons in a magnetic vortex," Phys. Rev. Lett. **122**, 097202 (2019).
[27]M. S. Wolf, R. Badea, M. Tader, and J. Berezovsky, "Strong driving of a single coherent spin by a proximal chiral ferromagnet," Phys. Rev. B **96**, 014424 (2017).